Abnormal Thermal Instability of Al-InSnZnO Thin-Film Transistor by Hydroxyl-Induced Oxygen Vacancy at SiO_X/Active Interface

Guk-Jin Jeon, Junghoon Yang, Seung Hee Lee, Wooseok Jeong, and Sang-Hee Ko Park

***Abstract*— We scrutinized the barrier capability of SiO_X, plasma Al_2O_3 (P-Al_2O_3)/SiO_X, and SiN_X/SiO_X passivation layers (PLs) on the environmental stabilities of back-channel etched Al-doped InSnZnO (Al-ITZO) TFTs at 85 °C with a relative humidity of 85 % for 30 days. Turn-on voltage (V_{ON}) of SiN_X/SiO_X-passivated TFTs was dramatically shifted to the negative direction and became conductive. Compared to those of SiO_X and P-Al_2O_3/SiO_X films, more hydroxyl groups existed at the PL/active interface of SiN_X/SiO_X-passivated Al-ITZO films. Water vapor transmission rates showed that abnormal behavior was not attributed to barrier capability of PL against the water vapor. When all TFTs were kept at 85 °C for 30 days in an air-drying oven, only the V_{ON} of SiN_X/SiO_X-passivated TFTs shifted negative direction and finally became conductive. Secondary ion mass spectroscopy (SIMS) results revealed that this abnormal behavior originates from the formation of oxygen vacancy due to highly existed hydroxyl group at SiO_X/Active interface at an elevated temperature.**

***Index Terms*— Al-doped InSnZnO (Al-ITZO) TFT, SiN_X/SiO_X passivation layer, oxygen vacancy, hydroxyl groups.**

I. Introduction

AMORPHOUS oxide semiconductors (AOS) have drawn much attention due to their many advantages such as high mobility, uniformity, stability, and application to the diverse electronic devices [1]–[7]. Among them, the high-mobility of oxide thin film transistors (TFTs) is very important for realizing high-resolution of active matrix-type electronic devices, not only for displays but for diverse sensors [8]. Despite their demands, achieving high-mobility oxide TFTs with excellent environmental stability is still challenging.

Manuscript received December 17, 2020; revised January 20, 2021; accepted January 23, 2021. Date of publication January 27, 2021; date of current version February 24, 2021. This work was supported by the National Research Foundation of Korea (NRF) Grant funded by the Korean Government under Grant 2018R1A2A3075518 and Grant 2020R1A6A3A13061266. The review of this letter was arranged by Editor P. Barquinha. *(Guk-Jin Jeon and Junghoon Yang contributed equally to this work.) (Corresponding author: Sang-Hee Ko Park.)*

The authors are with the Department of Materials Science and Engineering, Korea Advanced Institute of Science and Technology, Daejeon 34141, South Korea (e-mail: shkp@kaist.ac.kr).

Color versions of one or more figures in this letter are available at https://doi.org/10.1109/LED.2021.3054859.

Digital Object Identifier 10.1109/LED.2021.3054859

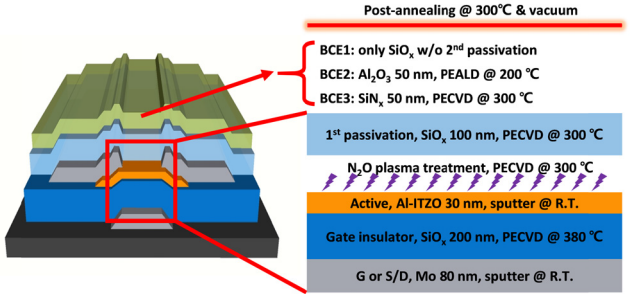

Fig. 1. Process procedure to fabricate Al-doped InSnZnO BCE TFT with various passivation layers.

In the case of a high-mobility oxide TFT, the device characteristics can be significantly affected by the passivation process [9], [10].

Typically, SiO_x and SiN_x deposited by plasma-enhanced chemical vapor deposition (PECVD) are widely used as passivation materials of oxide TFTs. Many research groups have studied the effect of the passivation process on the electrical performance of InGaZnO (IGZO) TFTs. Although the barrier capability of SiO_x is generally poorer than that of SiN_x, it is a common practice to use SiO_x in oxide TFTs as a first passivation layer (PL) due to the control of V_{on}. For both excellent barrier capability and electrically stable device performance, a double-stacked layer, such as SiN_x/SiO_x, has been investigated for the passivation of IGZO TFTs [11], [12]. However, the performance of oxide TFT is significantly affected by the hydrogen, especially during the SiN_x deposition [13]. Despite these findings, there were no related reports about the effects of external heat and/or water on the electrical stability of Al-doped InSnZnO (Al-ITZO) TFTs, which is one of the promising channel materials for high-mobility oxide TFTs, with SiN_x/SiO_x double passivation layer [14].

In this study, we observed a dramatic negative shift of turn-on voltage (V_{on}) of Al-ITZO TFT with SiN_x/SiO_x PL under high temperature and humidity. To clarify the origin of this abnormal behavior, the relationship between the TFT characteristics and PL was investigated by decoupling the moisture and heat.

II. Experiment

Fig. 1. shows all of our TFT fabrication processes. We fabricated BCE-structured high mobility Al-ITZO with three different PLs such as a SiO_x, each pair of P-Al_2O_3/SiO_x layers and SiN_x/SiO_x layers. Firstly, An 80 nm-thick Mo film was deposited on a glass substrate by sputtering and patterned into a gate electrode. SiO_x film with a thickness of 200 nm was deposited at a temperature of 380 °C to prevent H diffusion from the GI into the active layer during post-annealing. The deposition of an Al-ITZO active layer was conducted by sputtering with an Ar:O_2 ratio of 7:3, followed by wet patterning. A Mo film was deposited by sputtering and patterned to form a source and drain electrode. The back surface of all TFTs was treated with N_2O plasma in a PECVD chamber to reduce the carrier concentration of the backchannel before deposition of a PL.

SiO_x PL with a thickness of 100 nm was formed in situ via PECVD at 300 °C using N_2O and SiH_4 gases. Some of the TFTs with SiO_x PL were transferred into the ALD chamber and Al_2O_3 film with a thickness of 50 nm was deposited as a second PL by plasma ALD (P-Al_2O_3) using trimethylaluminum and O_2 plasma. Some of the TFTs with SiO_x PL were passivated by a 50 nm-thick SiN_x film by PECVD using NH_3 and SiH_4 gases. All TFTs were post-annealed at 300 °C under vacuum for 2 hours.

The electrical performances of all TFTs were characterized with a semiconductor parameter analyzer (4156A; Agilent). SiO_x/Al-ITZO/SiO_x (BCE1), P-Al_2O_3/SiO_x/Al-ITZO/SiO_x (BCE2), and SiN_x/SiO_x/Al-ITZO/SiO_x (BCE3) were deposited separately on a Si wafer. The films were analyzed via secondary ion mass spectroscopy (SIMS; IMS 7f; CAMECA). X-ray photoelectron spectroscopy (XPS) analyses were performed using a Sigma Probe (Thermo VG Scientific). The BCE1, 2, and 3 stacks were deposited for SIMS and XPS analysis subjected to the same annealing processes as the TFTs.

To analyze environmental stability, all TFTs were stored at a temperature of 85 °C and relative humidity of 85 %. The channel width/length of TFTs measured after 85 °C and 85 % stress and 85 °C stress was 40 μm/20 μm and 40 μm/40 μm, respectively. To analyze barrier capability, passivation film/Al-ITZO stacks were deposited on a polyimide substrate with low barrier capability. The water vapor transmission rates (WVTRs) of the films were measured by an AQUATRAN Model 1 instrument (MOCON).

III. Results and Discussion

To evaluate the environmental stability of TFTs with various PLs, all TFTs were stored in a chamber under a temperature of 85 °C and a relative humidity of 85% for 30 days. As shown in Fig. 2(a)~(c), the stability of each TFT varied significantly depending on the PL. Interestingly, the initial V_{on} of BCE3 TFTs was shifted more negatively compared to those of other ones due to the increased doing of H during the SiN_x deposition. In the BCE1 and BCE3 TFTs, each V_{on} was negatively shifted. The transfer characteristics of BCE1 TFT showed a hump after 5 days. The poor barrier of SiO_x PL allows water vapor diffusion into the oxide semiconductor to increase the carrier concentration in the backchannel due

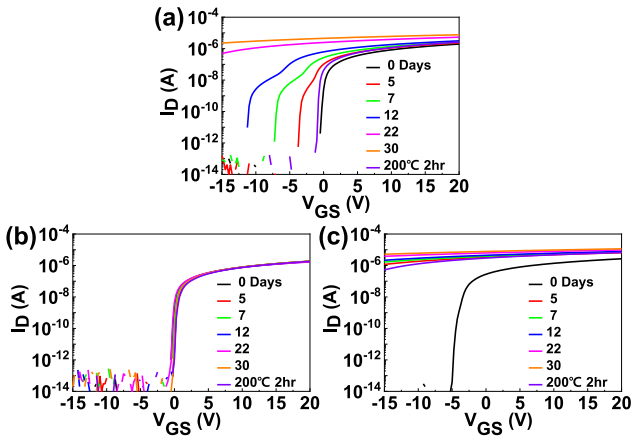

Fig. 2. Stability of Al-ITZO TFTs with (a) SiO_x (BCE1), (b) P-Al_2O_3/SiO_x (BCE2), and (c) SiN_x/SiO_x (BCE3) PLs at temperature of 85 °C and a relative humidity of 85 %. The drain voltage during the measurement of transfer characteristics was 0.1 V. The channel width and length have 40 μm and 20 μm, respectively.

to the electron doping effect of water molecules [15]. This increase of the carrier density induces the formation of a back channel, resulting in the hump. The hump gradually increased over time but the transfer characteristics almost recovered to their initial state after post-annealing at 200 °C under vacuum due to out-diffusion of water from the active layer. As shown in Fig. 2(a), a single SiO_x PL could not protect Al-ITZO TFT from the permeation of water under a high-humidity environment. Meanwhile, the V_{on} shift in the BCE2 TFT was 0.5 V, even after 30 days due to the robust barrier capability of the P-Al_2O_3 second PL (Fig. 2(b)). The TFTs with the P-Al_2O_3 PL showed highly stable performance under high temperature and humidity. On the other hand, the BCE3 TFT shows an abrupt negative V_{on} shift after 5 days, as illustrated in Fig. 2(c). The BCE3 TFT was not recovered to its initial state even after post-annealing at 200 °C in a vacuum. SiN_x film is known to be an excellent barrier to water and/or hydrogen, so it is difficult to conclude that this abrupt shift in BCE3 occurred by the permeation of water.

Since the passivation layer can affect the backchannel of the active layer, XPS analysis was performed to investigate the chemical bonding states at the passivation/active interface. As shown in (Fig. 3(a)~(c)), we deconvoluted the O 1s peak and divided it into four Gaussian curves to analyze the presence of O-related species [16]–[18]. The area ratios of the M-O, V_o, and OH peaks shown in Fig. 3(d) indicate the relative concentrations of three O components. In the PL/active interface, the O 1s peaks of BCE1, BCE 2, and BCE3 have the OH ratios of 25.45, 19.23 and 40.93 %, respectively. Compared to those of BCE1 and BCE2, the OH ratio of BCE3 is significantly higher. The OH ratio can be increased when interstitial H (H_i) combines with O, which indicates the increase of weakly bonded oxygen species [19], [20]. Therefore, the dramatic negative V_{on} shift of BCE3 TFT can be attributed to an increase of hydroxyl groups.

To exclude the barrier capabilities of the PLs from the origin of the abnormal V_{on} shift at 85 °C, we measured their WVTRs (not shown here). The SiO_x, P-Al_2O_3/SiO_x, and SiN_x/SiO_x PLs had WVTR values of 0.282, 0.054, and 0.186 g/m^2 day, respectively, after 60 hours and the WVTRs of all films satu-

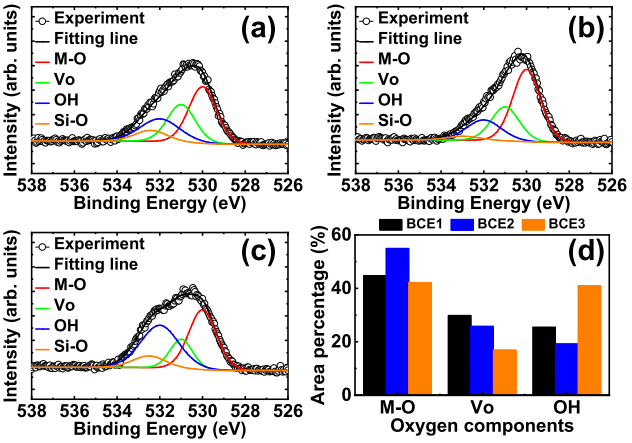

Fig. 3. XPS results of Al-ITZO with (a) SiO_X (BCE1), (b) P-Al_2O_3/SiO_X (BCE2), and (c) SiN_X/SiO_X (BCE3) PLs. (d) the area ratios of oxygen species such as M-O, V_O, and OH, respectively.

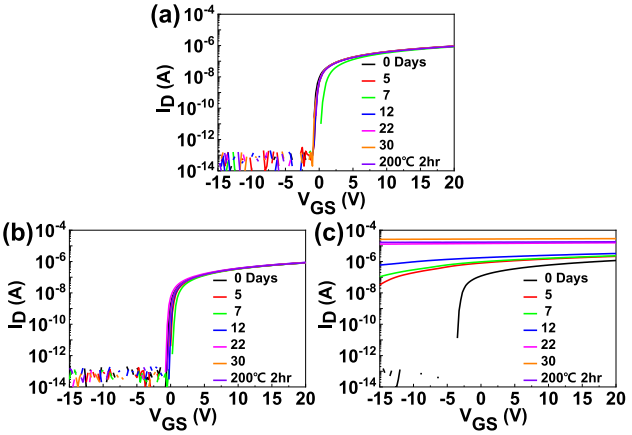

Fig. 4. Stability of Al-ITZO thin-film transistors with (a) SiO_X (BCE1), (b) P-Al_2O_3/SiO_X (BCE2), and (c) SiN_X/SiO_X (BCE3) PLs at a temperature of 85 °C in an air-drying oven. The drain voltage during the measurement of these characteristics was 0.1 V.

rated. The application of the Al_2O_3 film improved the barrier capability by almost a factor of 10 compared to that of a single SiO_X film. Meanwhile, the WVTR results also showed a higher barrier capability for the SiN_X/SiO_X film than the SiO_X film, which suggests that the abrupt V_{on} shift of BCE3 not caused by only the permeation of water, but can be attributed to the combined effect of high humidity and temperature conditions. Therefore, all TFTs were stored for 30 days at 85 °C in an air-drying oven. As shown in Fig. 4, the transfer characteristics of the BCE1 and BCE2 TFTs showed no significant changes over the 30 days period (Fig. 4(a)∼(b)). The V_{on} of BCE3 TFT, however, shifted dramatically in the negative direction after just 5 days and its transfer curve shows metallic characteristics (Fig. 4(c)). This confirms that the dramatic V_{on} shift of the BCE3 TFT was due to the heat.

To determine the origin of the V_{on} shift caused by heat, the BCE2 and BCE3 films were analyzed by SIMS (Fig. 5). The BCE2-85 and BCE3-85 films were stored for 16 days at 85 °C in the air-drying oven, and compared to those stored at room temperature (BCE2-RT and BCE3-RT). For both BCE2 and BCE3, the amount of H decreased over the entire region of the active layer (Fig. 5(a)). Assuming that H acts as a shallow donor, the reduction of H content would not be directly related to the negative V_{on} shift.

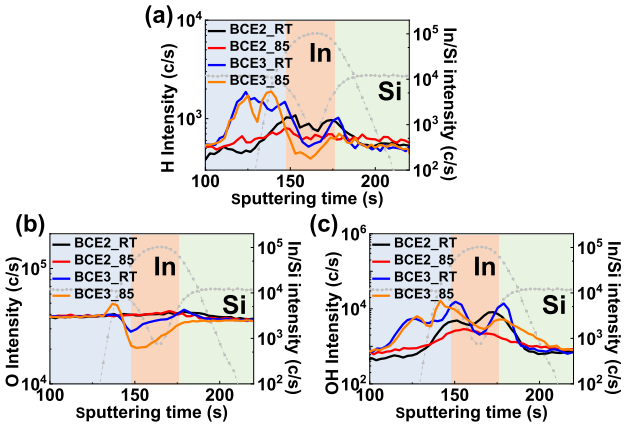

Fig. 5. SIMS depth profiles for the (a) hydrogen and (b) oxygen (c) hydroxyl group of BCE2 and BCE3 films before (RT) and after storage at 85 °C. The blue, orange, and green regions indicate the SiO_X PL, Al-ITZO active layer and SiO_X gate insulator, respectively.

On the other hand, the O content of the BCE2 and BCE3 films showed different results before and after storage at 85 °C (Fig. 5(b)). While the amount of O in BCE2 did not change, that of O in the BCE3 decreased over the entire region of the active layer after storage at 85 °C, as did H. The reduction of O content can cause an increase of V_o in the active layer. Since some of V_o act as an intrinsic donor in amorphous oxide semiconductors, it induces an increase in carrier density, resulting in a negative V_{on} shift as shown in Fig. 4(c). Since both the O and OH content in the active layer decreased in BCE3, we suggest that highly existed hydroxyl groups can induce the formation of oxygen vacancies by the reaction with the extra H (Fig. 5(b)∼(c)), as reported previously [21]. This suggestion is very consistent with the previous XPS results, as shown in (Fig. 3(a)∼(d)).

IV. Conclusion

In this work, we suggested that the origin of abnormal thermal instability for the Al-InSnZnO thin-film transistor with SiN_X/SiO_X PL. SiO_X PL layer with poor barrier performance could not prevent water incorporation into the active layer to yield degraded V_{on} characteristics. To improve this poor barrier property, we applied the SiN_X/SiO_X PLs to the Al-ITZO TFT. Nevertheless, to our surprise, the TFT with SiN_X/SiO_X PLs showed huge a negative V_{on} shift under the thermal effect. According to the conventional mechanism, the negative V_{on} shift had to be attributed to the role of the shallow donor by the diffusion of external H. However, the Al-ITZO TFT passivated by SiN_X/SiO_X contains relatively high portion of hydroxyl group in active layer due to the H incorporation during the SiN_X deposition. At an elevated temperature, it seems to be vulnerable to generate V_o from the reaction of M-OH and H^+ to yield water and V_o.

Unlike the existing concept of the passivation layer, which only emphasizes the role of preventing the permeation of external water or oxygen, this study provides a new perspective that the V_o induced by internally generated hydroxyl groups can degrade TFT stability.

REFERENCES

[1] K. Nomura, H. Ohta, A. Takagi, T. Kamiya, M. Hirano, and H. Hosono, "Room-temperature fabrication of transparent flexible thin-film transistors using amorphous oxide semiconductors," *Nature*, vol. 432, no. 7016, pp. 488–492, Nov. 2004, doi: 10.1038/nature03090.

[2] H. Yabuta, M. Sano, K. Abe, T. Aiba, T. Den, H. Kumomi, K. Nomura, T. Kamiya, and H. Hosono, "High-mobility thin-film transistor with amorphous $InGaZnO_4$ channel fabricated by room temperature RF-magnetron sputtering," *Appl. Phys. Lett.*, vol. 89, no. 11, Sep. 2006, Art. no. 112123, doi: 10.1063/1.2353811.

[3] D. Hong and J. F. Wager, "Passivation of zinc-tin-oxide thin-film transistors," *J. Vac. Sci. Technol. B, Microelectron. Nanometer Struct. Process., Meas., Phenomena*, vol. 23, no. 6, pp. L25–L27, Nov./Dec. 2005, doi: 10.1116/1.2127954.

[4] Y.-L. Wang, F. Ren, W. Lim, D. P. Norton, S. J. Pearton, I. I. Kravchenko, and J. M. Zavada, "Room temperature deposited indium zinc oxide thin film transistors," *Appl. Phys. Lett.*, vol. 90, no. 23, Jun. 2007, Art. no. 232103, doi: 10.1063/1.2746084.

[5] E. Fortunato, P. Barquinha, A. Pimentel, L. Pereira, G. Gonçalves, and R. Martins, "Amorphous IZO TTFTs with saturation mobilities exceeding 100 cm^2/Vs," *Phys. Status Solidi RRL*, vol. 1, no. 1, pp. R34–R36, Jan. 2007, doi: 10.1002/pssr.200600049.

[6] M. K. Ryu, S. Yang, S.-H.-K. Park, C.-S. Hwang, and J. K. Jeong, "High performance thin film transistor with cosputtered amorphous Zn–In–Sn–O channel: Combinatorial approach," *Appl. Phys. Lett.*, vol. 95, no. 7, Aug. 2009, Art. no. 072104, doi: 10.1063/1.3206948.

[7] J. H. Song, K. S. Kim, Y. G. Mo, R. Choi, and J. K. Jeong, "Achieving high field-effect mobility exceeding 50 cm^2/Vs in In-Zn-Sn-O thin-film transistors," *IEEE Electron Device Lett.*, vol. 35, no. 8, pp. 853–855, Aug. 2014, doi: 10.1109/LED.2014.2329892.

[8] T. Kamiya, K. Nomura, and H. Hosono, "Present status of amorphous In–Ga–Zn–O thin-film transistors," *Sci. Technol. Adv. Mater.*, vol. 11, no. 4, Feb. 2010, Art. no. 044305, doi: 10.1088/1468-6996/11/4/044305.

[9] S.-H. K. Park, M.-K. Ryu, H. Oh, C.-S. Hwang, J.-H. Jeon, and S.-M. Yoon, "Double-layered passivation film structure of Al_2O_3/SiN_x for high mobility oxide thin film transistors," *J. Vac. Sci. Technol. B, Nanotechnol. Microelectron., Mater., Process., Meas., Phenomena*, vol. 31, no. 2, Mar. 2013, Art. no. 020601, doi: 10.1116/1.4789423.

[10] S.-H.-K. Park, J. W. Kim, M.-K. Ryu, J.-E. Pi, C.-S. Hwang, and S.-M. Yoon, "Bilayered etch-stop layer of Al_2O_3/SiO_2 for high-mobility In–Ga–Zn–O thin-film transistors," *Jpn. J. Appl. Phys.*, vol. 52, no. 10, Oct. 2013, Art. no. 100209, doi: 10.7567/JJAP.52.100209.

[11] M. D. H. Chowdhury, M. Mativenga, J. G. Um, R. K. Mruthyunjaya, G. N. Heiler, T. J. Tredwell, and J. Jang, "Effect of SiO_2 and SiO_2/SiN_x passivation on the stability of amorphous indium-gallium zinc-oxide thin-film transistors under high humidity," *IEEE Trans. Electron Devices*, vol. 62, no. 3, pp. 869–874, Mar. 2015, doi: 10.1109/TED.2015.2392763.

[12] J. S. Jung, K.-H. Lee, K. S. Son, J. S. Park, T. S. Kim, J. H. Seo, J-H. Jeon, M.-P. Hong, J.-Y. Kwon, B. Koo, and S. Lee, "The effect of passivation layers on the negative bias instability of Ga–In–Zn–O thin film transistors under illumination," *Electrochem. Solid-State Lett.*, vol. 13, no. 11, pp. H376–H378, Aug. 2010, doi: 10.1149/1.3481710.

[13] D. H. Kang, J. U. Han, M. Mativenga, S. H. Ha, and J. Jang, "Threshold voltage dependence on channel length in amorphous-indium-gallium-zinc-oxide thin-film transistors," *Appl. Phys. Lett.*, vol. 102, no. 8, Feb. 2013, Art. no. 083508, doi: 10.1063/1.4793996.

[14] S. H. Cho, J. B. Ko, M. K. Ryu, J.-H. Yang, H.-I. Yeom, S. K. Lim, C.-S. Hwang, and S.-H.-K. Park, "Highly stable, high mobility Al: SnZnInO back-channel etch thin-film transistor fabricated using PAN-based wet etchant for source and drain patterning," *IEEE Trans. Electron Devices*, vol. 62, no. 11, pp. 3653–3657, Nov. 2015, doi: 10.1109/TED.2015.2479592.

[15] J.-S. Park, J. K. Jeong, H.-J. Chung, Y.-G. Mo, and H. D. Kim, "Electronic transport properties of amorphous indium-gallium-zinc oxide semiconductor upon exposure to water," *Appl. Phys. Lett.*, vol. 92, no. 7, Feb. 2008, Art. no. 072104, doi: 10.1063/1.2838380.

[16] M. D. H. Chowdhury, J. G. Um, and J. Jang, "Remarkable changes in interface O vacancy and metal-oxide bonds in amorphous indium-gallium-zinc-oxide thin-film transistors by long time annealing at 250 °C," *Appl. Phys. Lett.*, vol. 105, no. 23, Dec. 2014, Art. no. 233504, doi: 10.1063/1.4903874.

[17] S. Yoon, Y. J. Tak, D. H. Yoon, U. H. Choi, J.-S. Park, B. D. Ahn, and H. J. Kim, "Study of nitrogen high-pressure annealing on InGaZnO thin-film transistors," *ACS Appl. Mater. Interfaces*, vol. 6, no. 16, pp. 13496–13501, Aug. 2014, doi: 10.1021/am502571w.

[18] M. Chun, J. G. Um, M. S. Park, M. D. H. Chowdhury, and J. Jang, "Effect of top gate potential on bias-stress for dual gate amorphous indium-gallium-zinc-oxide thin film transistor," *AIP Adv.*, vol. 6, no. 7, Jul. 2016, Art. no. 075217, doi: 10.1063/1.4960014.

[19] M. D. McCluskey, M. C. Tarun, and S. T. Teklemichael, "Hydrogen in oxide semiconductors," *J. Mater. Res*, vol. 27, no. 17, pp. 2190–2198, Sep. 2012, doi: 10.1557/jmr.2012.137.

[20] J. K. Jeon, J. G. Um, S. Lee, and J. Jang, "Control of O-H bonds at a-IGZO/SiO_2 interface by long time thermal annealing for highly stable oxide TFT," *AIP Adv.*, vol. 7, no. 12, Dec. 2017, Art. no. 125110, doi: 10.1063/1.5008435.

[21] N. Domingo, E. Pach, K. Cordero-Edwards, V. Pérez-Dieste, C. Escudero, and A. Verdaguer, "Water adsorption, dissociation and oxidation on $SrTiO_3$ and ferroelectric surfaces revealed by ambient pressure X-ray photoelectron spectroscopy," *Phys. Chem. Chem. Phys.*, vol. 21, no. 9, pp. 4920–4930, Feb. 2019, doi: 10.1039/C8CP07632D.